Volume 1 Issue 1 September 2023

REFLECTION

Journal home page: https://www.sdcjournal.in/index.php/reflection

Research Article

Timing and Spectral Analysis of Thermonuclear X-ray Burst from LMXB 4U 1636-536

Sarath Mohan, Susmitha Bose, Aromal P and Marykutty James*

St. Thomas College, Ranni, Pazhavangadi P.O, Pathanamthitta, 689673

*Corresponding author (*E-mail address*: marykuttykjames@yahoo.co.in)

Received: 19/10/2022, Received in revised form: 26/07/2023, Accepted: 28/08/2023

Abstract

Here we are presenting the results of Thermonuclear X-ray burst of 4U1636-536 using ASTROSAT/LAXPC data during the year 2017. Light curve analysis of this source reveals 12 thermonuclear X-ray burst like events. All the bursts are very strong and the burst peak to persistent intensity < 9 times except two burst B2 and B10. Energy resolved burst profile shows the burst like event disappear above 30 keV. We fitted each burst in different energy range with model BURS and found that the decay time decreases with energy. For the spectral analysis, nH value was frozen to $0.25\times 10^{22} atoms\ /cm^{2.}$ Time resolved spectral analysis shows that the flux and spectral data counts showed a maximum value at the peak time of each burst. The flux tends to show a decreasing manner after the peak time with respect to time duration.

Keywords: LMXB

1. Introduction

An X-ray binary system consists of a normal star transferring mass onto a compact object which might be a neutron star or a black hole. The compact object accretes matter from the companion through Roche lobe overflow or through stellar wind accretion. X-ray binaries can be classified into two classes according to the mass of the companion star. High Mass X-ray Binaries (HMXBs) which have companion star with solar mass 10 and Low Mass X-ray Binaries (LMXBs) which have the companion star with a mass of about one solar mass.

LMXB are bright X-ray sources which accrete through the Roche lobe overflow through the inner Lagrangian point. Neutron stars in this system have a low magnetic field 107 to 109 and matter does not fall on magnetic poles. X-rays in this system are produced at the inner part of the accretion disk and at the surface of the neutron star. X-rays are also produced from an extended region of above and below the disk and are called accretion disk corona. X-ray variabilities which are mostly observed by LMXBs are X-ray bursts and QPOs.

X-ray spectral changes can be studied by Color - Color Diagram (CCD). It is the plot of high energy hardness ratio vs. low energy hardness ratio. LMXBs are classified into two based on the shape in CCD diagram as Atoll and Z source. Z sources exhibited three branched shapes roughly forming a Z shape track in CCD. Horizontal branch, Normal branch and Flaring branch. Atoll source shows different branches like Island state, banana state etc. Few properties of LMXBs are X-ray eclipses and Dips and Thermonuclear X-ray Bursts [1].

Thermonuclear X-ray bursts (Type-I) manifest as a sudden increase in the X-ray intensity of accreting neutron stars. It is characterized by short rise time (0.5 - 5 s) and large decay time (10 - 100 s) and it is in an exponential manner [2]. These events are caused by unstable burning of accreted matter. The occurrence of these bursts is explained by a thermonuclear flash model. It explains that the accreted matter contains Hydrogen which falls on the surface of the neutron star from the disk and forming a layer several meters thick. It starts burning and form a He layer. Unstable burning of Helium results in thermonuclear bursts. After between ∼1 and several tens of hours, the temperature and density at the base of the layer become high enough that the fuel ignites, burning unstably and spreading rapidly to consume all the available fuel on the star in a matter of seconds. Such bursts have been observed to date from more than 70 sources. Observation of X-ray bursts helps to determine the neutron star radius if the distance to the source is known. Here we are analysing the Type-1 bursts from the low mass X-ray binary 4U 1636-536.

4U 1636-536 is a Low Mass X-ray Binary discovered with OSO-8. It is one of the persistent X-ray sources in our galaxy and it normally changes its state between hard and soft. Its distance is estimated at 6 kpc. Optical photometry revealed over a period of 3.8 hr and the companion star has a mass of 0.4 solar mass. Super bursts [3] and millisecond Quasi Periodic oscillations [4] were detected in this source. Doublet and rare triplet bursts were detected from this source [5] the AstroSat/LAXPC observed during 2016. Burst oscillations at ∼581 Hz are observed with 4–5σconfidence in three of these X-ray bursts [6]. 2019 and 2018 Astrosat data reveals it consists of 31 thermonuclear bursts five doublets and triplets. Burst with shortest recurrence time 3.8 min also obtained in this time [7].

1.1 Observation Data Reduction

Astrosat is India's first dedicated multi wavelength astronomy satellite. The satellite consists of five payloads. LAXPC has the largest effective area and sensitivity among all the missions flown so far in search of X-ray sources above 20 keV. LAXPC consists of three identical proportional counters named LAXPC10, LAXPC20, LAXPC30 with a total effective area of 8000 cm^2 at 5-30 keV.

Here we analyse theAstroSat LAXPC observations of low mass X-ray binary 4U1636-536 during the year 2017. The data from these sources 4U1636-536 are publicly available from the three detectors LAXPC10, LAXPC20 & LAXPC30 and the later one was switched off during the time of observation. Here, we analyzed three sets of data observed during 28 February 2017 & 21-22 June 2017 & 2 October 2017.

Observation ID	Time of Observation
G06_104T01_9000001060	28-Feb-2017
G07_040T01_9000001326	21-Jun-2017
A04_055T01_9000001574	02 & 03 Oct-2017

- 20170228_G06_104T01_9000001060_level1/laxpc contains 14 orbits.
- 20170621_G07_040T01_9000001326_level1/laxpc contains 9 orbits.
- 20171002_A04_055T01_9000001574_level1/laxpc contains 15 orbits.

1.2 Timing Analysis of 4U 1636-536

For the data reduction of the source 4U 1636-536 we used the software developed by IUCAA. To analyse the LAXPC data, we have to create level2 event files. *laxpc_make_filelist* tool used for the creation of eventfiles and filterfiles. The eventfiles are used for producing a file called *'level2.event.fits'* by using laxpc_make_event*eventfiles* command. The GTI file, *usergti.fits, which* has the Good Time Intervals that removes earth occultation and SAA, with *laxpc_make_stdgti*command as a filter file as input. For further analysis we make use of the *level2.event.fits* file and the *usergti.fits* file.

The command *laxpc_make_lightcurve used* to produce light curves. The parameters associated with this command are -p, -t, -u and -o, -p represents the LAXPC counter we are considering for creating a particular light curve. Here, we use -p 12, indicating the consideration of first and second PCUs and not the third (since the). Binning time is specified by -t and output filename by -o, -u indicates GTI file which has eliminated the South Atlantic Anomaly (SAA) and certain gaps in space astronomy. The default energy range of light curves produced will be 3 to 80 keV. But a different energy to our convenience can be given to the file *eneinput* by editing it can create for different energy ranges. These light curves contain the information of source and background.

First and foremost, we created and plotted a light curve for bin time 1 s with 3-80 keV and identified a total of 12 thermonuclear bursts or burst like events. It is necessary to remove the background radiation from the lightcurve created. This can be done by creating a background light curve alone and subtracting it from the total light curve. The tool to make a background lightcurve is *laxpc_make_backlightcurve* with parameters -u, -p and -t with the same values as mentioned above. The subtraction of background from the source light curve can be done by using *lcmath* tool. The resultant light curve was of the source excluding the background, to plot this we use *lcurve* tool. This process was done in all three sets of data.

The light curve is a graph which shows the brightness of an object for a period of time and can be obtained by binning the events in the aspect of time. Light curves from the observation Id 9000001060 hereafter we call L1 given in Figure 1. It showed three Type 1 bursts or bursts like events and was denoted as B1, B2 and B3. Light curves from the observation Id 9000001326 hereafter we call L2 and given in Figure 2; which showed 3 burst like events. The last set of data from the observation Id 9000001574 hereafter we call L3 given in Figure 1.3 and showed 6 Type 1 bursts. All of these 12 showed a fast linear rise and exponential decay profile as in Type-1 Bursts. All these light curves are plotted in 1s bin time.

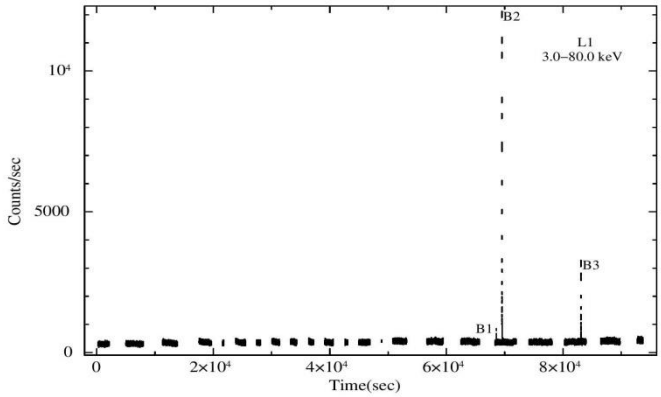

Figure 1: Light curve during the time MJD 17812 0:04 to 17813 2:02 plotted with 1s bin time in 3.0- 80.0 keV energy band from 4U 1636-536 using AstroSat/LAXPC data

To analyse the burst profile we fitted all the 12 bursts with model *constant (CO) and BURS*. Here the CO model is used to fit the persistent part and the burst region can be fitted with the BURS (it is a combination of fast rise and exponential decay) model. The below figures (Figure 4, Figure 5 and Figure 6) show the fitted burst profile and the fitted parameters specified in Table 1, 2 and 3.

The atoll source 4U 1636-536 shows a persistent count rate of ~ 500 c/s. 18th segment of the light curve shows two burst and 20th segment shows one. The first burst B1 is smaller compared to the other two. The peak count rate of the burst B1 reached ~800 c/s, and decayed in 5.23 sec. Burst duration of the B1 burst is 7.043 s. The second burst B2 is very strong and has a count rate of ~12200 c/s. Burst B3 has a peak count rate of ~3200 c/s. Burst duration of the B2 and B3 are 8.45 s and 7.16 s respectively. Average decay time of the burst is around 5.023 seconds. The separation time between B1 and B2 is ~930 s and between B2 and B3 is ~ 3.7586 hrs.

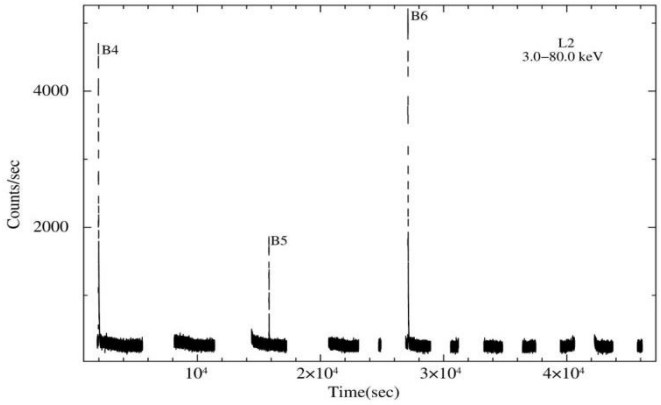

Figure 2: Light curve during the time MJD 17925 15:31 to 17926 3:48 plotted with 1s bin time in 3.0- 80.0 keV energy band from 4U 1636-536 using AstroSat/LAXPC data

Figure 2 shows the light curve the Observation ID 9000001326. Total of12 segments in the light curve. From the figure, it is clear that, first, third and sixth segments of light curve show a burst. These three Type-1 X -ray bursts are denoted as B4, B5 & B6 hereafter in this paper. The persistent count rate is ~680 counts/second. The intensity of B4 (1st segment) raised upto~4050 counts/second. B5 (3rd segment) showed a rise of ~1500 counts/second and for B6 (6th segment) ~ 4700 counts/second. After the sudden rise, an exponential decay to persistent

level was also observed. The separation between B4 & B5 is 3.824 hours, and that for B5 & B6 is 3.12 hours.

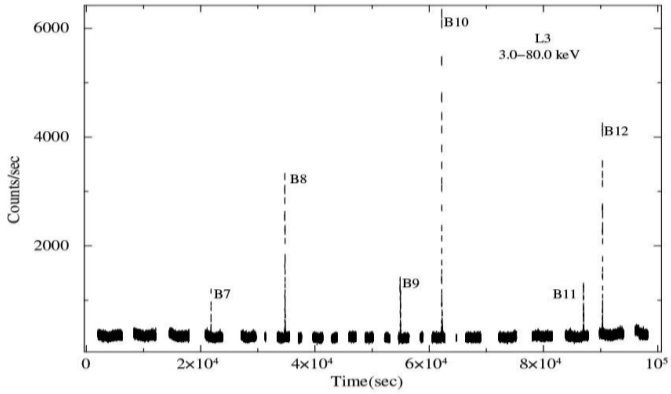

Figure 3 : Light curve during the MJD 18028 6:34 to 18029 9:17 plotted with 1s bin time in 3- 80 keV energy band from 4U 1636-536 using AstroSat/LAXPC data

The light curve L3 shows six Type-1 bursts denoted by B7, B8, B9, B10, B11 & B12. The light curve consisted of 23 segments and the intensity of B7 (4th segment) raised upto ~875 counts/second. B8 (7th segment) showed a rise to ~3000 counts/second, while B9 (14th segment) is ~1000 counts/second. Intensity raise in B10 (16th segment), B11 (21st segment) and B12 (22nd segment) are to ~6000 counts/second, ~900 counts/second and ~4000 counts/second respectively. B8 appears 12911 seconds after B7. B8 and B9 have 20154 seconds, B9 and B10 have 7219 seconds, B10 and B11 have 24773 seconds, B11 and B12 have 3298 seconds of separation.

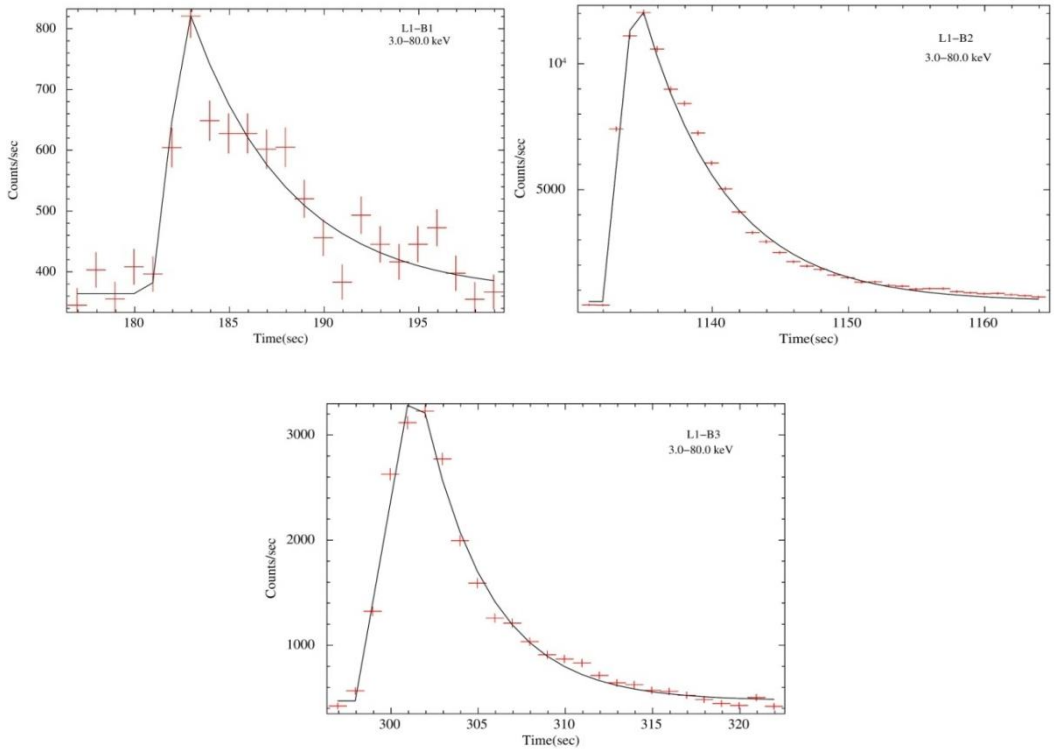

Figure:4 Bursts detected (B1, B2 and B3) of L1 fitted using the model BURS.

Table 1.1: Fitted parameters of the observed Type I bursts in L1 from the source 4U1636-536 using LAXPC 20 data.

Burst No.	Rising Time	Decay Time	Burst	Persistent	Peak Count	Ratio of
B1	1.813	5.23	7.043	364.01	480.00	1.318
B2	2.37	6.08	8.45	550.00	12750.00	23.182
B3	3.40	3.76	7.16	471.95	3198.03	6.78

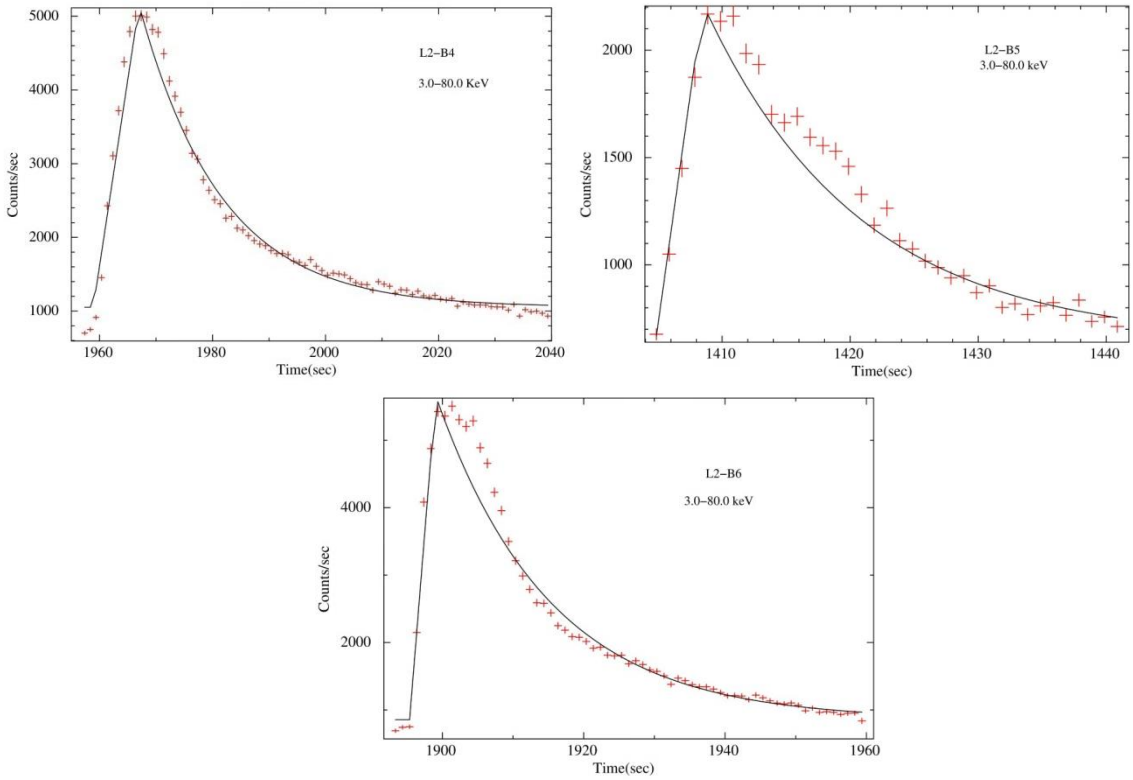

Figure:5 Bursts detected (B4, B5 and B6) of L2 fitted using model CO and BURS.

Table 1.2: Fitted parameters of the observed Type I bursts in L2 from the source4U1636-536 using the of LAXPC 20.

Burst No.	Rising Time (s)	Decay Time (s)	Burst Duration (s)	Persistent Count Rate (counts/s)	Peak Count Rate (counts/s)	Ratio of Peak to Persistent Count rate
B4	8.0	14.47	22.47	1052	4100	3.897
B5	3.0	12.10	15.1	646.0	1570	2.430
B6	4.0	16.0	20.0	856.5	4800	5.604

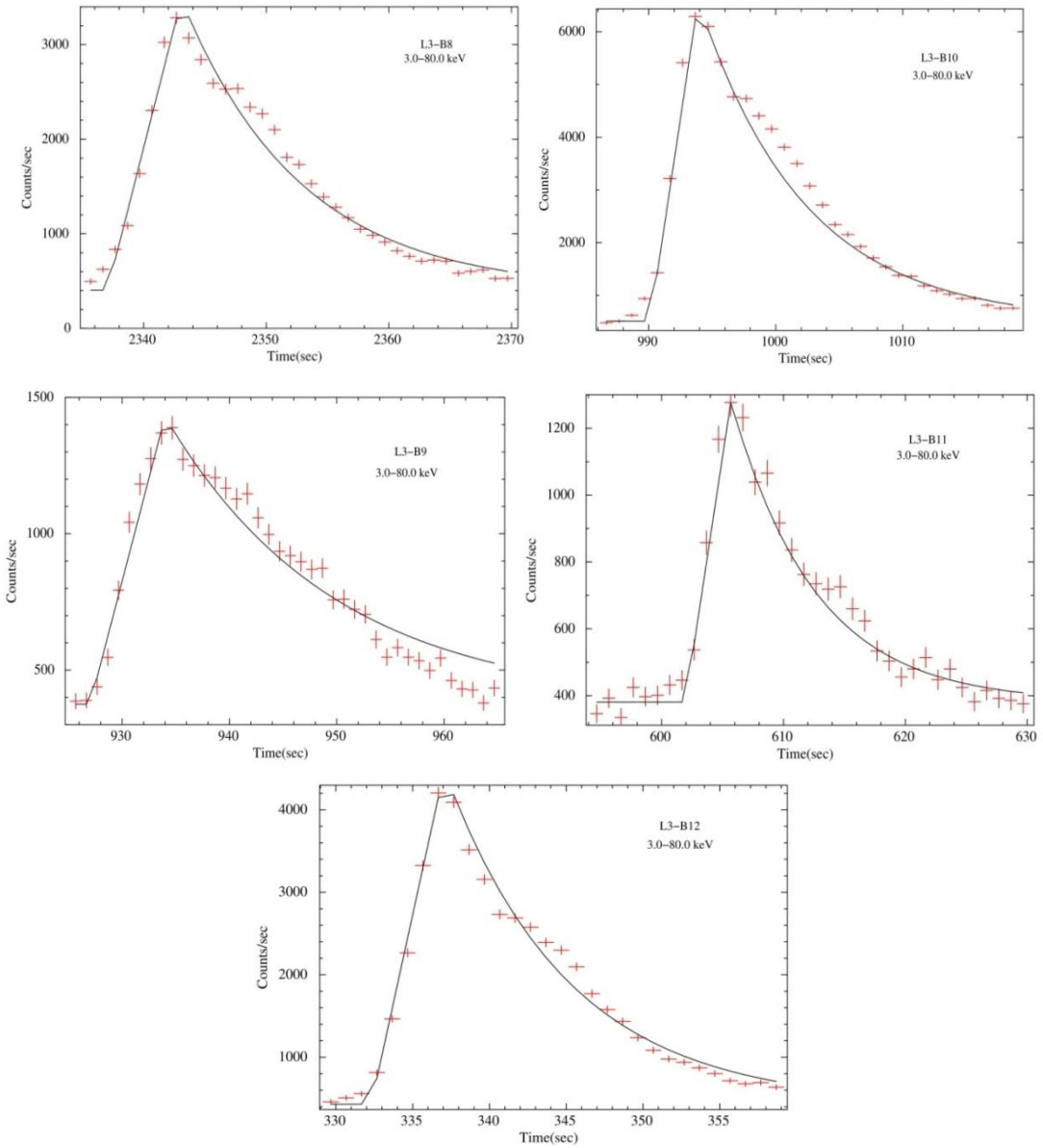

Figure: 6: Bursts detected (B7, B8, B9, B10, B11 and B12) of L3 fitted using model BURS. Best fit parameters are given in the corresponding table.

Table 3: Fitted parameters of the observed Type I bursts in L3 from the source 4U1636-536 using LAXPC 20 data

Burst No.	Rising Time	Decay Time	Burst Duration (s)	Persistent Count Rate	Peak Count Rate	Ratio of Peak to Persistent Count
B7	3.300	2.363	5.663	333.8	875.0	2.621
B8	6	9.713	15.713	404.1	3075	7.609
B9	7	15.75	22.75	375.0	1055	2.813
B10	3.8	8.318	12.118	512.8	6080	11.85
B11	3.7	6.904	10.604	380.6	900	2.3646
B12	4.8	8.038	12.838	431.4	4050	9.388

1.2.1 Energy Dependence of Burst Profile

To check the energy dependence of the burst profile, we created the burst-like event in different energy ranges. For the analysis we used the background subtracted data from LAXPC 20. The energy ranges were 3.0-6.0 keV, 6.0-9.0 keV, 9.0-15.0 keV, 15.0-20.0 keV, 20.0-25.0 keV and 25.0-30.0 keV except in some cases. The combined plots of burst profiles for different energy ranges are given below in Figure 7, Figure 8 and Figure 9.

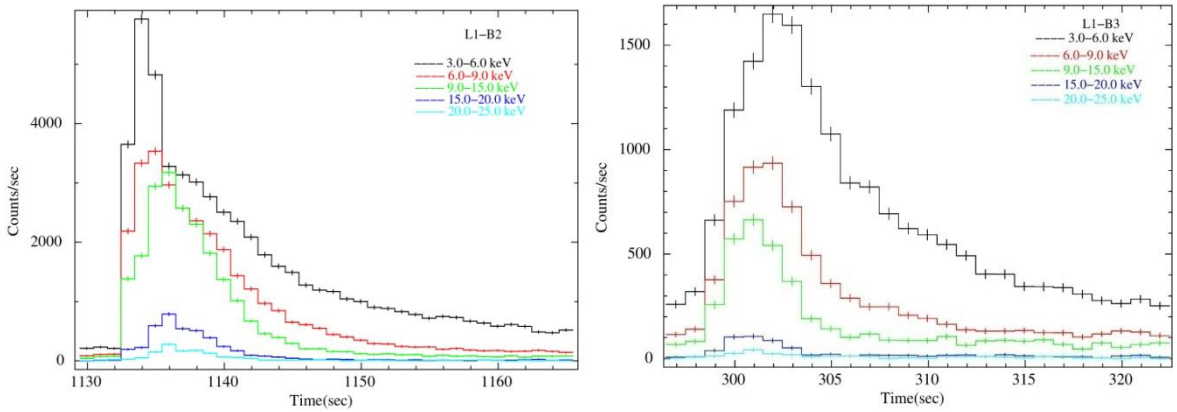

Figure 7: Energy resolved burst profiles (B2 & B3) of L1 from 4U1636-536 showing a decreasing peak count rate at higher energy bands.

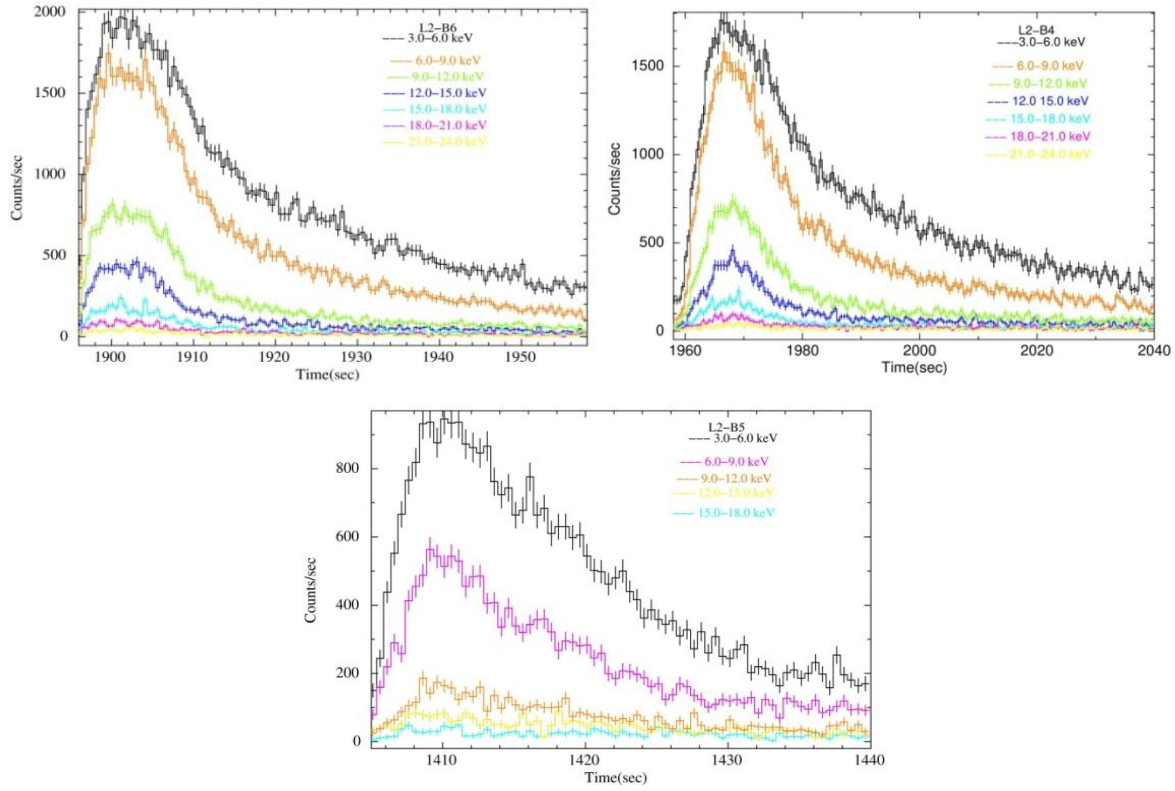

Figure 8: Energy-resolved burst profiles (B4, B5 & B6) of L2 from 4U1636-536 showing a decreasing peak count rate at higher energy bands.

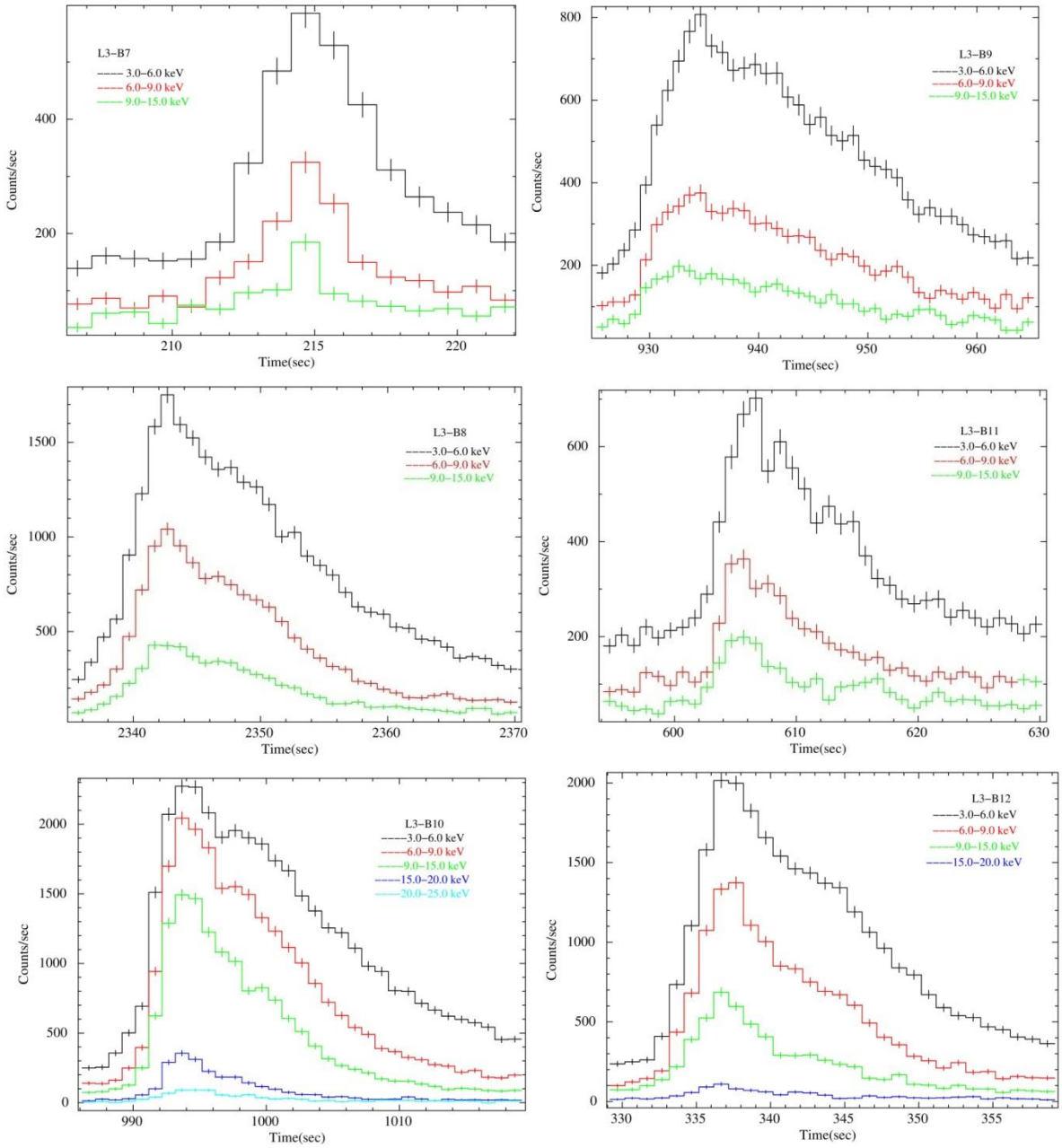

Figure 9: Energy-resolved burst profiles (B7, B8, B9, B10, B11 & B12) of L3 from 4U1636-536 showing a decreasing peak count rate at higher energy bands.

We can see the decreasing count rate with increasing energy in the energy resolved burst profiles of B2 to B12. B1 is not shown, as it does not show any energy dependence since the burst is too small, compared to other 11 bursts. The count rate is maximum for 3.0-6.0 keV in all energy-resolved burst profiles. In Type I burst B7, B8, B9 and B11, the burst region is indistinguishable above 15.0 keV.

Another important observation from energy dependence plots is the variation of decay time with energy. It is seen that the decay time decreases as the energy increases. To study this variation, energy-resolved plots of B3, B6 & B10 are fitted using model BURS. The plot of energy v/s decay time is plotted and is given in Figure 10.

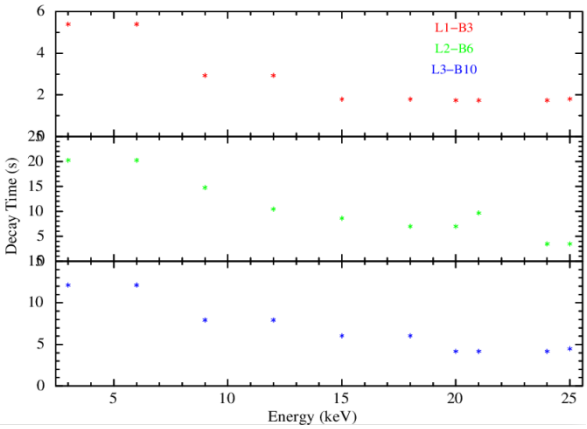

Figure 10: Energy vs Decay Time of L1:B3, L2:B6 and L3:B10 from 4U1636-536showing a decreasing decay time at higher energy band

1.3: Spectral Analysis

To carry out the spectral analysis, we created source spectra and back ground spectra with tool *laxpc_make_spectra and laxpc_make_backspectra*. For all the spectral analysis, we used the data from LAXPC20. In all spectral analysis we add a systematic error of 3.0 percent. Spectrum gives a plot of the background subtracted spectra with energy (in keV) on the x-axis and normalized counts (in /sec/keV) on the y-axis. We created each spectrum for an energy range from 4.0 to 20.0 keV and were later fitted using standard models available in *XSPEC* The flux (in ergs/cm^2/s) of each spectrum was found by using the command '*flux 4 20'* and the variation of flux was observed.

Forall the spectral fitting, we have to use certain multiplicative models like absorption model (*tbabs)*, and additive models blackbody spectrum *(bbodyrad)*, *powerlaw*:simple photon power law, accretion blackbody components *(diskbb)* and gaussian line profile model: *gaussian*. These models together with their respective parameters gave the perfect fit for the corresponding spectrum. The perfect fitting was found by checking and minimizing the reduced chi-squared value which in turn minimizes the error of a given spectra. To perform the fitting of a respective spectrum, we froze the value of equivalent Hydrogen column density (nH) to $0.25\ X10^{22} atoms\ /cm^2$ as that obtained from the nH calculator to find the perfect fit.

1.3.1 Time resolved spectral analysis

Time-resolved spectral analysis is important for the study of the evolution of the spectra. During the thermonuclear burst, the spectral properties are changing. The second burst of the first light curve (L1 B2), the third burst of the second light curve (L2 B6) and the fourth burst of the third light curve (L3 B10) were selected for the time-resolved (due to high intensity) spectral analysis.

For L1-B2 we have created a total of eight independent background subtracted spectra for the energy range 4.0-20.0 keV using LAXPC 20. Spectrum for rising time, peak time and decay time were created individually; among which the decay region is splitted into five segments. The XSPEC models *tbabs, bbodyrad, diskbb and powerlaw* using the command were used to fit the spectrum. By using the reduced chi squared method we found the perfect fit for

each spectrum and froze the value of equivalent hydrogen column density *nH*as $0.25\times 10^{22} atoms\ /cm^2$ as obtained from the nH calculator. The flux (in ergs/cm^2/s) of each spectrum was found. Spectral data counts varied from 1777.24 c/s to 28686 c/s. The parameters that were observed by doing the spectral fitting of L1 B2 are shown in Table 4 below.

Table 4: Spectral parameters observed for L1- B2 detected from 4U1636-536 using LAXPC 20, in the time-resolved spectral analysis.

	L1-B2: Burst Time							
	Burst 1-4	Burst 5-7	Burst 8-12	Burst 13-17	Burst 18-22	Burst 23-27	Burst 28-32	Burst 33-35
kTin (keV)	$1.52^{+0.08}_{-0.108}$	$1.95^{+0.14}_{-0.09}$	$2.14^{+0.06}_{-0.08}$	$1.41^{+0.06}_{-0.08}$	$1.09^{+0.08}_{-0.10}$	$3.03^{+1.93}_{-0.81}$	$0.72^{+0.14}_{-0.20}$	$1.41^{+0.45}_{-0.37}$
Norm	$225.97^{+39.31}_{-84.83}$	$186.9^{+64.4}_{-102.8}$	$90.7^{+29.65}_{-20.27}$	$232.3^{+37.17}_{-29.44}$	$377.3^{+136.5}_{-84.4}$	$0.61^{+2.62}_{-0.52}$	1536.7	$25.14^{+119.2}_{-17.38}$
Diskbb-Tin	$4.02^{+3.99}_{-1.01}$	$4.86^{+3.51}_{-1.03}$	-	$4.77^{+12.2}_{-1.61}$	-	$1.33^{+0.13}_{-0.15}$	$2.41^{+0.87}_{-0.50}$	-
Diskbb-Norm	$1.24^{-1.34}_{-1.30}$	$2.86^{-2.60}_{-2.37}$	-	$0.21^{+2.00}_{-0.21}$	-	$116.0^{+91.8}_{-41.8}$	$2.95^{+7.46}_{-2.00}$	-
Pho. Index	-	-	$2.08^{+0.407}_{-0.41}$	-	$3.25^{+2.26}_{-0.88}$	-	-	$3.59^{-3.68}_{-1.18}$
Norm	-	-	$3.57^{+4.29}_{-2.31}$	-	$0.80^{+2.06}_{-0.60}$	-	-	$11.12^{-12.9}_{-12.1}$
Flux (ergs/cm^2	1.3869 e-08	4.6423 e-08	2.4911 e-08	8.0772e-09	4.0208 e-09	2.522e-09	2.0236 e-09	1.7972e-09
Spectral Data	13004.4	28686	24317.5	10207.1	6173.7	5400.93	4048.19	1777.24
Reduced Chi	0.576	0.680625	1.019375	1.772	0.7561	0.723125	1.486	1.215

Figure 1 shows a maximum flux of 4.6423 e-08 ergs/cm^2/s for the peak time in the burst region L1-B2, and the decrease in the flux was observed as the time evolved. The spectral data counts variation with time was plotted, the burst region of 33-35 seconds showed the minimum spectral data counts of 1777.4c/s and the maximum spectral data counts of 28686 c/s was for the burst region of 5-7 seconds.

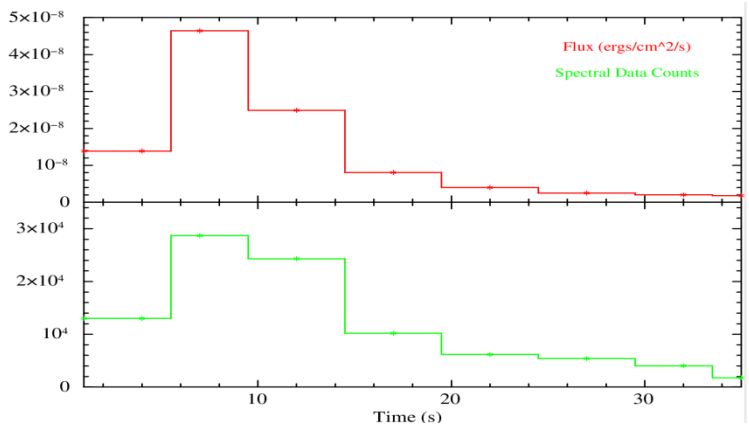

Figure 11: Plot showing variation of Flux (ergs/cm^2/s) & Spectral Data Counts with time in L1 B2 detected from 4U1636-536 using LAXPC, performing XSPEC model fitting in the time-resolved spectral analysis.

L2-B6 has 57 seconds of duration for which the above mentioned models were used and the perfect fit was found; the nH value was frozen to $0.25\times 10^{22} atoms\ /cm^2$. We have split the burst region into 9 segments and individual spectra were created. Mostly, the models *tbabs*, *bbodyrad*and *powerlaw*gave the best fit; but in the region of 27 to 33 seconds *tbabs*, *bbodyrad* together with *diskbb*gave the reduced chi squared value for the perfect fit. The parameters that were observed by doing the spectral fitting of L2 B6 are shown in Table 1.5 below.

Table 5: Fitting parameters observed for L2 B6 detected from 4U1636-536 using LAXPC 20, in the time-resolved spectral analysis.

Model	L2-B6 : Burst Time								
	Burst 1-4	Burst 5-8	Burst 9-12	Burst 13-18	Burst 19-26	Burst 27-33	Burst 34-40	Burst 41-47	Burst 48-57
kTin (keV)	$2.02^{+0.14}_{-0.07}$	$2.01^{+0.11}_{-0.08}$	$1.97^{+0.1}_{-0.06}$	$1.70^{+0.07}_{-0.05}$	$1.49^{+0.08}_{-0.06}$	$1.42^{+0.10}_{-0.09}$	$1.35^{+0.09}_{-0.09}$	$1.23^{+0.11}_{-0.14}$	$1.35^{+2.89}_{-0.78}$
Norm	$69.45^{+14.44}_{-22.67}$	$94.92^{+23.25}_{-28.04}$	$100.14^{+16.26}_{-27.2}$	$113.6^{+16.03}_{-30.53}$	$106.05^{+21.49}_{-39.26}$	$105.05^{+25.71}_{-21.13}$	$97.2^{+26.04}_{-18.90}$	$93.03^{+40.95}_{-45.06}$	$22.08^{+34.89}_{-16.43}$
Diskbb-Tin	-	-	-	-	-	$8.84^{+3.51}_{-9.14}$	-	-	-
Diskbb-Norm	-	-	-	-	-	$0.021^{+0.07}_{-0.01}$	-	-	-
Pho. Index	$1.18^{+0.86}_{-1.15}$	$1.54^{+0.64}_{-2.07}$	$1.18^{+0.86}_{-1.14}$	$1.13^{+0.91}_{-1.13}$	$1.45^{+0.77}_{-1.61}$	-	$1.03^{+0.77}_{-1.12}$	$1.63^{+0.65}_{-0.89}$	$2.17^{+0.35}_{-0.57}$
Norm	$0.15^{+1.38}_{-0.14}$	$0.62^{+1.97}_{-0.41}$	$0.167^{+1.58}_{-0.15}$	$0.102^{+0.89}_{-0.10}$	$0.20^{+1.13}_{-0.20}$	-	$0.052^{+0.25}_{-0.05}$	$0.25^{+0.27}_{-0.25}$	$1.01_{-1.02.}$
Flux (ergs/cm^2	1.25 e-08	1.792 e-08	1.58 e-08	9.593 e-9	5.756 e-09	4.34 e-09	3.385 e-9	2.756 e-9	2.248 e-9
Spectral Data	8612.2	14863.9	13413.3	12574.1	9534.51	7643.92	6372.28	5378.71	6310.47
Reduced Chi	1.1	1.1	0.6	1.15	0.6	1.55	1.29	0.64	1.1

In Figure 12 maximum flux 1.792 e-08(ergs/cm^2/s) was observed in the peak region of the burst 5-8 seconds and the maximum spectral data count for the 5-8 second region and minimum spectral count for 41-47 seconds.

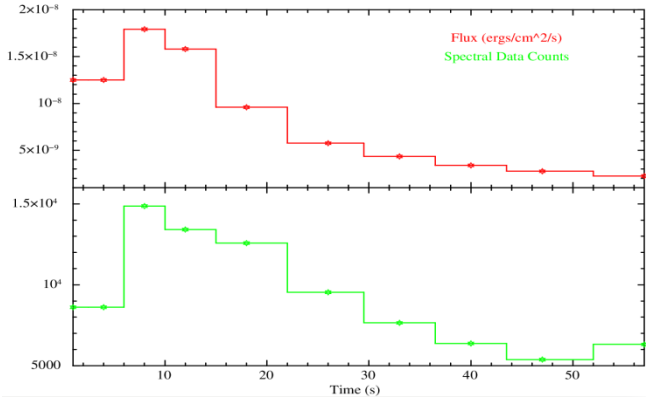

Figure 12: Plot showing variation of Flux (ergs/cm^2/s) & Spectral Data Counts with respect to time in L2 B6 detected from 4U1636-536 using LAXPC 20, in the time-resolved spectral analysis.

In the burst L3-B10 we have also added the XSPEC model *gaussian (*which gives a simple gaussian line profile), for the burst segment 9-12, 13-16 and 17-20. The other regions of the burst were fitted using the models as mentioned above; we froze the value of hydrogen column density *nH*as $0.25\times 10^{22} atoms\ /cm^2$ as obtained from the nH calculator. The parameters that were observed by doing the spectral fitting of L3 B10 are shown in Table 1.6 below.

Table 6: Fitting parameters observed for L3 B10 detected from 4U1636-536 using LAXPC 20, in the time-resolved spectral analysis.

L3-B10 : Burst Time									
	Burst 1-4	Burst 5-6	Burst 7-8	Burst 9-12	Burst 13-16	Burst 17-20	Burst 21-24	Burst 25-28	Burst 29-32
kTin (keV)	$2.04^{+0.65}_{-0.65}$	$1.96^{+0.28}_{-0.22}$	$2.02^{+0.12}_{-0.08}$	$2.75^{+14.61}_{-2.75}$	$2.27^{+0.18}_{-0.13}$	$2.33^{+0.33}_{-0.20}$	$1.12^{+0.17}_{-0.26}$	$1.22^{+0.28}_{-0.12}$	$1.60^{+0.40}_{-0.24}$
Norm	$3.64^{+21.6}_{-2.82}$	$33.8^{+33.22}_{-14.86}$	$103.8^{+27.9}_{-30.1}$	$13.50^{+13.53}_{-13.53}$	$39.8^{+17.5}_{-15.7}$	$17.0^{+12.65}_{-9.6}$	$233^{+346}_{-89.20}$	$94.07^{+85.4}_{-93.1}$	$33.5^{+69.9}_{-24.6}$
Diskbb-Tin	-	-	-	$2.82^{+0.37}_{-0.09}$	-	-	$3.05^{+1.00}_{-0.49}$	-	-
Diskbb-Norm	-	-	-	$13.29^{+1.02}_{-0.8}$	-	-	$2.28^{+5.27}_{-2.06}$	-	-
Pho. Index	$2.80^{+1.51}_{-0.83}$	$2.45^{+0.914}_{-0.91}$	$1.39^{+0.62}_{-1.36}$	-	-	-	-	$2.61^{+0.65}_{-1.34}$	$2.98^{+0.59}_{-0.69}$
Norm	$2.40^{+0.52}_{-0.48}$	$3.078^{+0.62}_{-0.58}$	$0.47^{+0.1}_{-0.02}$	-	-	-	-	$2.62^{+8.09}_{-1.70}$	$8.27^{+15.0}_{-6.47.}$
LineE	-	-	-	$6.98^{+0.96}_{-1.17}$	$4.36^{+0.89}_{-2.10}$	$3.78^{+1.03}_{-2.70}$	-	-	-
Sigma	-	-	-	$1.28^{+0.57}_{-0.84}$	$2.17^{+1.01}_{-0.64}$	$2.31^{+1.13}_{-0.62}$	-	-	-
Norm	-	-	-	$0.13^{+0.38}_{-0.22}$	$0.69^{+1.01}_{-0.33}$	$0.81^{+1.52}_{-0.37}$	-	-	-
Flux (ergs/cm^2	1.703 e-09	7.39 e-09	1.980 e-08	1.946 e-08	1.33 e-08	8.0191 e-09	4.61 e-09	3.085 e-09	4.447 e-09
Spectral Data	2670.4	4363.18	9946.84	16276.8	12337.5	8307.97	5465.95	4120.87	3217.68
Reduced Chi	0.6934	0.4375	0.6606	1.503	1.195	1.1013	1.149	1.372	1.402

In Figure 1.13 maximum flux 1.980e-08 in ergs/cm^2/s was observed for the peak time in the burst region 7-8 seconds and the spectral data counts varied from 2670 c/s to 16276 c/s. The flux tends to show a decreasing manner with respect to time.

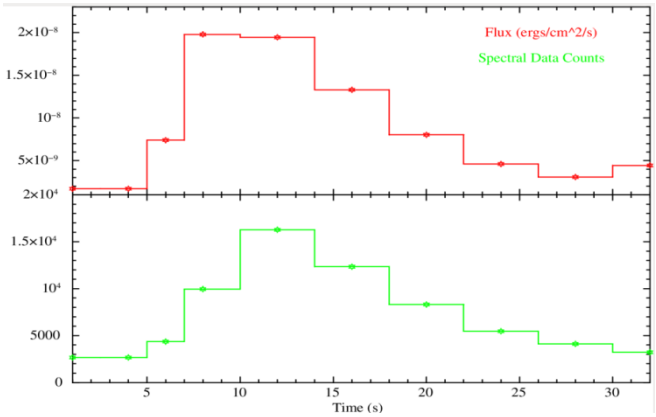

Figure 13.: Plot showing variation of Flux (ergs/cm^2/s) & Spectral Data Counts with time in L3 B10 detected from 4U1636-536 using LAXPC 20 in the time-resolved spectral analysis

1.3.2 Pre-Burst spectral analysis

To perform the Pre-Burst analysis, we have created *usergti* file of 30 seconds prior to the burst, of the high intensity bursts L1-B2, L2-B6 and L3-B10. With the *usergti* we created both source and background spectrum for each burst for the LAXPC20 and the background subtracted spectra were plotted for the whole burst in the energy band 4.0 to 20.0 keV. The models *Tbabs*(bbodyrad+diskbb)* was used to find the perfect fit for L1-B2, *tbabs*(bbodyrad+powerlaw)* was used to fit the spectrum for L2-B6 and L3-B10. As mentioned above, reduced chi squared technique was used to fit the spectrum accurately and the value of hydrogen column density *nH*was frozen to $0.25X10^{22} atoms\ /cm^2$. The fitted parameters for the pre burst spectral analysis observed for L1-B2,L2-B6 and L3 B10 detected from 4U1636-536 using LAXPC20 are shown in the table below.

Table 7: Fitting parameters observed for the 30 sec Pre-Burst region of L1-B2, L2-B6 & L3-B10 detected from 4U1636-536 using LAXPC20 in the spectral analysis.

Pre Burst: 30 sec			
Parameters	L1-B2	L2-B6	L3-B10
kTin (keV)	$2.42^{-3.96}_{-3.96}$	$1.35^{+0.33}_{-0.83}$	$1.577^{+0.477}_{-0.182}$
Norm	$1.24^{+1.57}_{-0.08}$	$7.13.^{+8.68}_{-7.52}$	$6.968^{+9.227}_{-5.503}$
Diskbb- Tin	$1.91^{+1.84}_{-1.80}$	-	-
Diskbb- Norm	$4.67^{-0.32}_{-0.29}$	-	-
Pho. Index	-	$1.42^{+0.47}_{-0.07}$	$2.170^{+0.453}_{-0.962}$
Norm	-	$0.087^{+0.05}_{-0.05}$	$0.327^{+0.629}_{-0.303}$
Flux (ergs/cm^2/s)	9.7538e-10	9.8117e-10	9.0701 e-10
Spectral data counts	1777.24	3430.6	11229.8
Reduced Chi Squared	1.011875	0.760625	1.268

1.3.3 Full Burst spectral analysis

The full burst spectrum is created as mentioned earlier. The flux and the spectral data counts were observed. Since we have used the models like *tbabs, bbodyrad, powerlaw and diskbb* we could find the parameters like kT (temperature in keV) temperature at inner disk radius (Tin), line energy (LineE), line width (Sigma), photon index (Pho.Index) and norm in different regions of spectrum of a X-ray source could be found by using the accurate fitting techniques. For the accurate fit; nH value was frozen to $0.25\times 10^{22} atoms\ /cm^2$ as mentioned above.

Table 8: Fitting parameters observed for the Full Burst region of L1-B2, L2-B6 & L3-B10 detected from 4U1636-536 using LAXPC20

Full Burst Region			
Parameters	L1-B2	L2-B6	L3-B10
kTin (keV)	$1.90^{+0.11}_{-0.09}$	$1.71^{+0.06}_{-0.04}$	$1.495^{+0.112}_{-0.137}$
Norm	$51.64^{+16.83}_{-12.50}$	$48.58^{+5.53}_{-12.3}$	$80.94^{+16.94}_{-27.18}$
Diskbb- Tin	-	-	$3.698^{+0.805}_{-0.476}$
Diskbb- Norm	-	-	$1.750^{+2.396}_{-0.979}$
Pho. Index	$2.40^{+0.19}_{-0.20}$	$1.72^{+0.30}_{-0.45}$	$9.499^{+10.0}_{-10.0}$
Norm	$4.67^{-0.32}_{-0.29}$	$0.49^{+0.69}_{-0.37}$	$1.719e-10$
Flux (ergs/cm^2/s)	1.0728 e-08	5.6684e-09	7.6102 e-09
Spectral data counts	71425.9	47048.6	51002.4
Reduced Chi Squared	0.93625	1.3925	1.1878

2.0: Results and Conclusion

The timing analysis of the bursting source 4U 1636-536 shows that, the light curves for the energy range 3.0-80.0 keV for the data during 28-Feb-2017, 21-Jun-2017 and 02 & 03 Oct-2017 using both LAXPC10 and LAXPC20 show 12 Thermonuclear Type I Burst like event. Pinaki Roy et al. 2022 also detected these bursts along with 2018 Astrosat data. The burst region showed a fast linear rise and exponential decay profile as in Type-1 Bursts. The Second burst B2 is very strong and has a count rate of~12200 c/s, has a count rate of ~ 4700 counts/second and B10 with count rate ~ 6080 counts/second. From the timing analysis, the burst duration of all bursts varies from 5.663 seconds to 22.75 seconds. In some sources like Cyg X-2 bursts are weak [8]; but all the bursts in this source are very strong and the burst peak

to persistent intensity <9 times except two burst B2 and B10. B2 have 21 times the peak intensity of the persistent rate and B 10 increased by a factor 11 times.

The energy-resolved analysis of the Type I burst shows a dependence up to 30.0 keV; above this energy range, the burst region becomes indistinguishable. As the energy increases, the count rate decreases in each burst. Decay time increases from 2.363 to 16.0 seconds in L1 to L3.

Time resolved spectral analysis is carried out in the three bursts (L1B2, L2B6 and L3 B10) which has highest count rate in each set. The burst duration divided into 8 segments and we fitted with conventional methods. Spectral analysis contained spectral fitting of the energy range 4 to 20 keV in which nH value was frozen to $0.25\times 10^{22} atoms\ /cm^{2.}$

Total burst spectrum also fitted with tbabs, diskbb, bbodyrad and power law. In these spectra, the black body temperature varying between 1.9 to 1.495 keV. From the 30 sec pre-burst spectrum, blackbody temperature varies between 2.42 -1.57. From the plot 12 and 13 reveals that the flux and spectral data counts showed a maximum value at the peak time of each burst. The flux tends to show a decreasing manner after the peak time with respect to time duration.

References

1. Walter H. G. Lewin and Jan van Paradijs and Edward P. J. van den HeuvelX-ray Binaries, Cambridge University Press, pp. 674.Cambridge, UK:1997
2. H. G Walter,Jan Lewin, Van Paradijs and Ronald E Taam X-Ray Bursts, Cambridge University Press, Cambridge Astrophysics Series, Cambridge, MA: |c1995, edited by Lewin, Walter H.G.; Van Paradijs, Jan; Van den Heuvel, Edward P.J.xrbi.nasa175L,1995.
3. Keek L., Cumming A.,Wolf Z, Ballantyne D R, Suleimanov V F, Kuulkers E and Strohmayer T. E. The imprint of carbon combustion on a superburst from the accreting neutron star 4U 1636-536. *Monthly Notices of the Royal Astronomical Society* 454 (4) (2015) 3559-3566.
4. Stiele H, Yu W. and Kong A.K.H. Millihertz Quasi periodic Oscillations in 4U 1636-536: Putting possible constraints on the neutron star size. *The Astrophysical Journal*, 831(1) (2016) 34S.
5. Aru Beri, Biswajith Paul, Yadav J S, Anita H M, Agarwal P. C et al. Thermonuclear X-ray bursts in Rapid succession 4U1636-536 using AstroSat/LACPC. *Monthly Notices of the Royal Astronomical Society*. 482 (4) (2019) 4397-4407.
6. Pinaki Roy, Aru Beri and Sudip Bhattacharya. Thermonuclear X-ray bursts from 4U 1636 - 536 observed with AstroSat. *Monthly Notices of the Royal Astronomical Society*. 508 (2) (2021) 2123-2133.
7. Pinaki Roy, Aru Beri and Mondal Adithya. NuSTAR and AstroSat observations of thermonuclear X-ray bursts with short-recurrence times in 4U 1636−536. *Journal of Astrophysics and Astronomy*. 43 (2) (2022).
8. Jincy Devasia, Gayathri Raman and Biswajit Paul Thermonuclear. X-ray bursts detected in Cyg X-2 using AstroSat/LAXPC. *New Astronomy*. 83 (2021) 101479